Published in final edited form as:

Nature. 2010 December 23; 468(7327): 1129–1132. doi:10.1038/nature09581.

Neurotransmitter/sodium symporter orthologue LeuT has a single high–affinity substrate site

Chayne L. Piscitelli[1,2,*], **Harini Krishnamurthy**[2,*], and **Eric Gouaux**[2,3]

[1]Department of Biochemistry and Molecular Biology, Oregon Health and Science University, 3181 SW Sam Jackson Park Road, Portland, Oregon 97239, USA

[2]Vollum Institute, Oregon Health and Science University, 3181 SW Sam Jackson Park Road, Portland, Oregon 97239, USA

[3]Howard Hughes Medical Institute, Oregon Health and Science University, 3181 SW Sam Jackson Park Road, Portland, Oregon 97239, USA

Abstract

Neurotransmitter/sodium symporters (NSSs) couple the uptake of neurotransmitter with one or more sodium ions[1–3], removing neurotransmitter from the synaptic cleft. NSSs are essential to the function of chemical synapses, are associated with multiple neurological diseases and disorders[4], and are the targets of therapeutic and illicit drugs[5]. LeuT, a prokaryotic orthologue of the NSS family, is a model transporter for understanding the relationships between molecular mechanism and atomic structure in a broad range of sodium-dependent and sodium-independent secondary transporters[6–13]. At present there is a controversy over whether there are one or two high-affinity substrate binding sites in LeuT. The first-reported crystal structure of LeuT, together with subsequent functional and structural studies, provided direct evidence for a single, high-affinity, centrally located substrate-binding site, defined as the S1 site[14,15]. Recent binding, flux and molecular simulation studies, however, have been interpreted in terms of a model where there are two high-affinity binding sites: the central, S1, site and a second, the S2 site, located within the extracellular vestibule[16]. Furthermore, it was proposed that the S1 and S2 sites are allosterically coupled such that occupancy of the S2 site is required for the cytoplasmic release of substrate from the S1 site[16]. Here we address this controversy by performing direct measurement of substrate binding to wild-type LeuT and to S2 site mutants using isothermal titration calorimetry, equilibrium dialysis and scintillation proximity assays. In addition, we perform uptake experiments to determine whether the proposed allosteric coupling between the putative S2 site and the S1 site manifests itself in the kinetics of substrate flux. We conclude that LeuT harbours a

Correspondence and requests for materials should be addressed to E.G. (gouauxe@ohsu.edu)..

*These authors contributed equally to this work.

Author Contributions C.L.P., H.K. and E.G. designed the research; C.L.P. and H.K. performed the research and analyzed the data; and C.L.P., H.K. and E.G. wrote the paper.

Supplementary Information is linked to the online version of the paper at www.nature.com/nature.

single, centrally located, high-affinity substrate-binding site and that transport is well described by a simple, single-substrate kinetic mechanism.

We first measured the thermodynamic response and stoichiometry of L-leucine binding to LeuT using isothermal titration calorimetry (ITC). To minimize the potential for artefacts in our binding assays arising from endogenously bound Leu co-purifying with LeuT, we extensively washed cell membranes with Na^+-free buffer containing the Na^+ chelator 15-crown-5[17]. For the wild-type LeuT–Leu interaction, ITC binding isotherms were best fitted by a single-site model with a substrate-to-LeuT stoichiometry, *N*, of 0.70±0.01 and a dissociation constant, K_d, of 54.7±1.8 nM (Fig. 1a and Supplementary Table 1). Binding of Leu to LeuT is driven by enthalpic and entropic factors with a ΔH of −3.93±0.02 kcal mol^{-1} and a −TΔS of −6.01±0.13 kcal mol^{-1}. Thermodynamic binding models of higher complexity describing two-site random- or sequential-binding modes yielded poorer fits to the data, with either high χ^2 values or non-converging parameters.

The measured stoichiometry, of 0.70, suggests that approximately 30% of LeuT in the ITC cell is unable to bind titrated substrate. This could be due to incomplete removal of endogenously bound substrate despite extensive `washing' of the membranes. To weaken substrate binding and thus diminish the relative proportion of Leu-bound LeuT, as well as to specifically probe the interaction of substrate with LeuT, we mutated Tyr 108 to Phe, thereby disrupting the hydrogen bond between the hydroxyl group of Tyr 108 and a carboxylate oxygen of substrate bound to the S1 site[14]. We proposed that by ablating the hydrogen bond between Tyr 108 and Leu, the Tyr 108 Phe mutation would reduce the enthalpy of Leu binding to the S1 site, thus allowing us to isolate apo-LeuT more readily.

Similar to the case for wild-type LeuT, the binding isotherm for Leu binding to the Tyr 108 Phe mutant was best fitted by a single-site model (Fig. 1b). Reflecting the predicted binding-site perturbation, the dissociation constant increased to K_d=1.4±0.1 μM; the stoichiometry parameter also increased (*N*=0.79±0.01) relative to the wild-type transporter (Supplementary Table 1). Notably, ΔH decreased to −1.92±0.03 kcal mol^{-1}, a difference of 2.01 kcal mol^{-1} from wild-type LeuT and consistent with the loss of a single hydrogen bond between LeuT and a single substrate molecule bound at the S1 site.

Because the stoichiometry values from the ITC experiments ranged from 0.7 to 0.8, we were compelled to determine how much residual substrate remained bound to LeuT. To measure the amount of `free' amino acid present in our LeuT samples, we employed quantitative amino-acid analysis (qAAA). The qAAA results (Supplementary Tables 2–7) show that the molar ratio of free Leu to LeuT is approximately 6% for Tyr 108 Phe but is negligible for the wild-type preparations. The presence of more free Leu in the Tyr 108 Phe preparations was unexpected and may be due to variations in individual membrane preparations as well as variability in qAAA determinations. Even if all of the free Leu is bound to LeuT, however, the fraction of LeuT bound with substrate does not fully account for the substoichiometric values obtained from ITC. Possible explanations for the substoichiometric binding of substrate are that the LeuT samples used in the experiments contain trace amounts of contaminating proteins, as judged by SDS–polyacrylamide gel electrophoresis (Supplementary Fig. 1), that there is a small amount of protein aggregation, as judged by

fluorescence-detection size-exclusion chromatography[18] (Supplementary Fig. 1), or that a fraction of LeuT is not competent to bind substrate.

To corroborate the binding parameters obtained by ITC, we used equilibrium dialysis to measure [^{3}H]Leu binding to LeuT. Data for wild-type LeuT and the Tyr 108 Phe mutant were well fitted by a single-site binding equation (Fig. 1c, d) with respective stoichiometries of 0.73±0.03 and 0.72±0.02 (Supplementary Table 1). Taken together, both the ITC and the equilibrium dialysis data are consistent with there being a single substrate-binding site. The observed differences between wild-type LeuT and Tyr 108 Phe demonstrate that we can use the LeuT crystal structure to perturb binding of substrate to the S1 site both specifically and predictably.

We next probed the presence of the S2 site by asking whether mutations in this proposed site would also measurably perturb binding of substrate to LeuT. In fact, it is claimed that mutation of Leu 400 to Cys ablates Leu binding to the S2 site, reducing overall binding to LeuT by approximately one-half[16]. We therefore measured [^{3}H]Leu binding to mutants Leu 400 Ala and Leu 400 Cys. Using equilibrium dialysis, we observed that the extent of Leu binding to Leu 400 Ala was comparable to that for the wild-type transporter (Fig. 1c and Supplementary Table 1). This conclusion was reinforced using the scintillation proximity assay (SPA) method[19] to compare [^{3}H]Leu binding with wild type, Leu 400 Ala and Leu 400 Cys (Fig. 2a). We find that neither the Leu 400 Ala nor the Leu 400 Cys mutant shows any significant change in Leu binding, as measured by maximum binding capacity or dissociation constant, relative to wild-type LeuT (Supplementary Table 1).

A limitation of the SPA method is the unreliable determination of the scintillant counting efficiency, which in turn complicates an accurate conversion of measured radioactivity in counts per minute to moles of radioligand. To circumvent the need for this transformation, we quantified the binding-site stoichiometry by titrating transporter protein at 20-fold excess over K_d with 0.06–3.0 molar equivalents of [^{3}H]Leu[20]. The resulting response is initially first order with respect to Leu concentration, as binding sites are in excess over ligand. When binding reaches saturation, binding is zeroth order with respect to Leu concentration. The intersection abscissa of the first-order and zeroth-order linear regressions provides the ligand concentration equivalent to the binding-site concentration, thus defining a stoichiometric value that is independent of ordinate radioactivity conversions. Using this method, we measured [^{3}H]Leu binding to wild-type LeuT and to the Leu 400 Ala and Leu 400 Cys mutants (Fig. 2b). For each of these transporters, binding-site saturation occurs at a nearly identical ligand concentration, each corresponding to a substrate-to-transporter stoichiometry of about 0.8, confirming that mutations at the Leu 400 position do not decrease the binding capacity of LeuT for Leu (Supplementary Table 1).

We performed a final saturation binding analysis to assess the effect of clomipramine, an inhibitor of LeuT transport[21],[22] that was proposed to displace Leu binding from the S2 site[16]. We saw no change in the binding of Leu to wild-type LeuT in the presence of 10nM LeuT and 1mM clomipramine, thus indicating that Leu- and clomipramine-binding sites do not overlap (Fig. 2c and Supplementary Table 1). This is consistent with previous data indicating that clomipramine is a non-competitive inhibitor of LeuT transport[21].

To augment our assessment of binding-site stoichiometry, we asked whether LeuT-catalysed transport is better modelled by a single-site kinetic model or one in which two substrates are bound. Previously reported flux measurements for several substrates showed that LeuT steady-state kinetics is well described by single-site Michaelis–Menten parameters. The overall slow turnover rate of LeuT under those conditions, however, may have obscured the detection of more complex kinetic behaviour. Here we sought to re-evaluate the kinetics of Ala transport under conditions tailored to promote higher turnover, to determine whether transport kinetics are better fitted by a one- or a two-site model. We first determined that uptake is more robust at low (acidic) pH values, with a maximum at pH 5, and that mutation of Lys 288, a residue protruding into the hydrophobic portion of the membrane bilayer[14], to Ala ($LeuT^K$) further enhanced substrate flux (Supplementary Fig. 2). Steady-state kinetics for Ala uptake by $LeuT^K$ under optimized conditions was measured in the presence of a 200mM inward Na^+ gradient. The data well fitted the Michaelis–Menten rectangular hyperbola with a Michaelis constant of K_m=0.79±0.06 μM and a maximal velocity of V_{max} = 11,006±281 pmol min^{-1} mg^{-1} (Fig. 3a). The corresponding turnover number is k_{cat}=0.65 min^{-1}, which is about sixfold higher than that measured for wild-type LeuT at pH 7 with a 100 mM Na^+ gradient[15] (Supplementary Table 8).

We reasoned that transport would be further stimulated by including valinomycin. Addition of this K^+-selective ionophore will induce a negative-inside membrane potential and prevent the build-up of positive charge inside the liposomes during transport. With valinomycin present, k_{cat} increased to 2.3 min^{-1} yet K_m remained nearly unchanged at 0.75±0.06 μM (Fig. 3b and Supplementary Table 8). Similar to transport under membrane-neutral conditions, valinomycin-stimulated transport is well fitted by a single-site Michaelis–Menten kinetic model.

In conjunction with the Michaelis–Menten modelling, the steady-state kinetic data were fitted with alternative kinetic models that describe kinetic mechanisms involving two binding sites: the Hill equation[23] for a random-order, cooperative-binding response; and a two-site, ordered-binding kinetic model[24]. Data fitted to the Hill equation converged with a Hill slope of n_H=0.96±0.03, indicating that there are not multiple interacting substrate sites underlying the kinetic behaviour of LeuT. A two-site, ordered-binding reaction scheme, which provides explicit treatment for both singly and doubly occupied transporter complexes[24], was fitted to the flux data. Although V_{max} was calculated to be 10,965±308 pmol min^{-1} mg^{-1}, which is nearly identical to the Michaelis–Menten model, the apparent dissociation constant, K_S, and the dissociation coefficient, α, converged to 6.8±22 nM and 114±360, respectively, indicating that the parameters are not well fitted by the data.

In conclusion, we have examined the stoichiometry of substrate binding to LeuT using multiple methods, and find consistent evidence for a single, high-affinity substrate-binding site. We find no evidence to support the notion that mutation of Leu 400 to Ala or Cys, or the presence of clomipramine, perturbs the stoichiometry of substrate binding. Furthermore, the kinetics of substrate flux is best fitted by a single-substrate kinetic model. Taken together, these data refute the two-substrate binding model for LeuT[16] and are consistent with previously determined crystallographic and functional data[14],[15],[21]. The mechanistic implications of our work are that transport of substrate by LeuT occurs through a singly

occupied intermediate where substrate is bound to a central, high-affinity site (the S1 site; Fig. 4). We maintain, however, that substrate may indeed transiently bind to weak, low-affinity sites as it transits from the extracellular solution to the S1 site and from the S1 site to the intracellular solution, as suggested by previous structural and computational studies[6,15].

METHODS SUMMARY

We washed membranes containing LeuT or mutants three times with buffer containing 50 mM Tris-HCl (pH 8.0) and 10 mM 1,4,7,10,13-pentaoxacyclopentadecane (15-crown-5)[17], and purified them as described in either ref. 14 (ITC and equilibrium dialysis)or ref. 16 (SPA). For ITC experiments[25], we determined the protein and Leu concentrations and the residual free-amino-acid content of purified LeuT by qAAA (Supplementary Tables 1–6). An extinction coefficient of 136,459 cm^{-1} M^{-1} was empirically determined by qAAA measurements of LeuT. We performed ITC experiments at 25 °C using an ITC_{200} calorimeter (MicroCal) with either 20 μM wild-type or 30 μM Tyr 108 Phe LeuT in the cell, and titrated with 200 μM or 500 μM L-Leu, respectively. Equilibrium dialysis experiments were performed by placing 100 μl of 60 nM wild-type LeuT, 94 nM Leu 400 Ala or 5.7 μM Tyr 108 Phe in the sample chamber of a Rapid Equilibrium Dialysis Device plate (Thermo Scientific) and 300 μl of [^{3}H]Leu at 0.3–30 μM in the buffer chamber. Saturation binding experiments using SPA were performed with 10 nM protein incubated with 2 mg ml^{-1} Cu^+-YSi SPA beads (GE Healthcare) in the presence of 0.3–600 nM [^{3}H]Leu. For measurement of binding-site concentration using SPA, we used 400 nM protein and 25–1,200 nM [^{3}H]Leu. For transport assays, LeuT proteoliposomes were prepared as previously described[14] in a 1:100 protein/lipid weight ratio. Transport assays were conducted at 27 °C with 10 μg ml^{-1} protein. To determine steady-state kinetic parameters, we allowed reactions to proceed for 2 min and quenched, filtered and analysed them using GRAPHPAD PRISM 4 as previously described[14].

METHODS

Mutagenesis and protein purification

Site-directed mutants of LeuT were prepared using PCR. The Tyr 108 Phe mutant of LeuT was made in the background of the Lys 288 Ala mutation (Tyr 108 Phe–$LeuT^K$). Wild-type LeuT and mutants bearing a carboxy-terminal His_8 tag were expressed in C41 cells and purified as previously described[14] with the exception that cell membranes were washed three times with 50 mM Tris-HCl (pH 8.0) supplemented with 10 mM 1,4,7,10,13-pentaoxacyclopentadecane (15-crown-5)[17] to facilitate the removal of bound Leu and augment the generation of apo-LeuT. Purified protein destined for equilibrium dialysis and ITC assays was concentrated to 5–30 μM using a concentrator with a 50-kDa cut-off, and dialysed at 4 °C for 24 h against buffer I (20 mM Tris-citrate (pH 7.0), 200 mM NaCl and 1 mM dodecyl maltoside), with three buffer changes. Protein for scintillation proximity assays was purified in buffer II[16] (150 mM Tris-MES (pH 7.5), 50 mM NaCl, 1 mM dodecyl maltoside and 20% glycerol). Equilibrium dialysis assays on wild-type LeuT demonstrate no notable differences using either buffer I or buffer II. Reducing conditions were maintained for preparations of the Leu 400 Cys mutant using 2 mM tris(2-carboxyethyl)phosphine (TCEP). The concentration of protein and ligand used in the ITC measurements was directly

determined by qAAA on material that was subjected to overnight acid hydrolysis in 0.02 N HCl. The extent to which the purified LeuT starting material was contaminated by residual Leu was determined by qAAA of non-hydrolysed material to measure the free-amino-acid content. All qAAA measurements were performed at the Keck Biotechnology Resource Laboratory at Yale University. All other protein concentrations were estimated by absorbance spectroscopy using a molar extinction coefficient of 136,459 cm^{-1} M^{-1} at λ = 280 nm for the His-tagged protein, derived from the extinction coefficient predicted from primary sequence (ProtParam; http://expasy.org/tools/protparam.html) and empirically corrected by qAAA measurements of LeuT (A_{280} of unity = 0.43 mg ml^{-1}). Sample purity was assessed by SDS–polyacrylamide gel electrophoresis under reducing conditions using 12.5% Tris-Gly gels (Supplementary Fig. 1a). Protein dispersity was monitored by fluorescence-detection size-exclusion chromatography[18] measuring intrinsic Trp fluorescence (Supplementary Fig. 1b).

Isothermal titration calorimetry

A solution of wild-type LeuT or Tyr 108 Phe-$LeuT^K$ (at 20 or 30 μM, respectively, in buffer I) was loaded into the sample cell of an ITC_{200} calorimeter (MicroCal). L-Leu at 200 or 500 μM for titrations with wild-type LeuT or Tyr 108 Phe–$LeuT^K$, respectively, was dissolved in buffer I and loaded into the injection syringe. Before data collection, the system was equilibrated to 25 °C with the stirring speed set to 1,000 r.p.m. Titration curves for Tyr 108 Phe–$LeuT^K$ binding Leu were generated by five successive 1.5-μl injections followed by fourteen 2.0-μl injections at 180-s intervals. Titration curves for wild-type LeuT binding Leu were generated with nineteen 2.0-μl injections at 180-s intervals. Control injections of ligand into buffer I without protein were done to determine background corrections. The integrated heats from each injection, normalized to the moles of ligand per injection, were fitted to a single-site binding isotherm[25] using ORIGIN 7. Final values of K_d, stoichiometry (N), ΔH and – TΔS were determined from the average of two to four ITC runs.

Equilibrium dialysis

For each replicate, 100 μl of either 60 nM wild-type LeuT, 94 nM Leu 400 Ala or 5.7 μM Tyr 108 Phe–$LeuT^K$ protein in buffer I was placed in the sample chamber of a Rapid Equilibrium Dialysis Device plate (Thermo Scientific) and 300 μl of [^{3}H]Leu at 0.3–30 μM (0.27 Ci $mmol^{-1}$) in buffer I was placed in the buffer chamber. The unit was covered with sealing tape and incubated at room temperature (23 °C) on a shaker for 6 h. To determine the concentrations of total and free ligands, 10-μl aliquots were removed from the sample and buffer chambers, respectively, and added to 6 ml of Ultima Gold scintillation fluid. The concentrations of free and total Leu were calculated from the tSIE (transformed spectral index of an external standard)-corrected d.p.m. (disintegrations per minute) values measured using a liquid scintillation counter. Data were analysed as a single-site binding function. Values of K_d, B_{max} (maximal binding) and N were determined from the average of two independent experiments, with two to four replicates each.

Scintillation proximity assays

For saturation binding analysis, 10 nM LeuT was incubated with 2 mg ml^{-1} Cu^{+}-YSi SPA beads in buffer II in the presence of 0.3–600 nM [^{3}H]Leu (10.8 Ci $mmol^{-1}$). The reactions were mixed on an orbital microplate shaker at room temperature. Plate readings were taken at 2, 20, 40 and 60 h using a Wallac Microbeta plate counter, although for each experiment no significant change was observed after 20 h incubation. SPA experiments to quantify the binding-site concentration in each sample were performed as described above, but using 400 nM LeuT and 25–1,200 nM [^{3}H]Leu (10.8 Ci $mmol^{-1}$). For all assays, specific binding was calculated by subtracting the background radioligand binding assessed by duplicate binding measurements in the presence of 5 mM L-Ala.

Transport time course

LeuT was reconstituted into lipid vesicles as previously described[14] using internal buffer appropriate for the experiment (20 mM HEPES-Tris (pH 7), 200 mM KCl or 20 mM citrate-Tris (pH 6, pH 5 or pH 4) and 200 mM KCl). Transport reactions were assembled by diluting LeuT proteoliposomes to a final protein concentration of 10 μg ml^{-1} in external buffer (20 mM HEPES-Tris (pH 7.0), 200 mM NaCl or 20 mM citrate-Tris (pH 6.0, pH 5.0 or pH 4.0) and 200 mM NaCl) at 27 °C with 500 nM [^{3}H]Ala (83 Ci $mmol^{-1}$). Uptake was followed by removing and quenching 100-μl aliquots of the reaction in ice-cold internal buffer at various time points up to 40 min. Reactions were filtered and analysed as previously described[14]. Non-specific uptake was assessed by repeating the time course for the same liposome preparation under identical conditions except for the replacement of external NaCl by KCl. Non-specific uptake was then subtracted from the total uptake measured to calculate the specific uptake. Each experiment was performed in duplicate.

Steady-state kinetics

LeuT proteoliposomes at 10 μg ml^{-1} were incubated with 0.050–8.0 μM [^{3}H]Ala (8.3 Ci $mmol^{-1}$) at 27 °C for 2 min in external buffer (20 mM citrate-Tris (pH 5.0) and 200 mM NaCl) with or without 50 nM valinomycin. Preliminary time course experiments done with 0.050, 0.40, 1.0 and 8.0 μM [^{3}H]Ala established that transport remained linear through the 2-min time point. Data from two to four experiments, each repeated in duplicate, were fitted to the Michaelis–Menten equation and analysed by linear regression to an Eadie–Hofstee transformation.

To test for multisite cooperative kinetics, data were modelled according to the Hill equation, $v = (V_{max}[S]^n)/(K' + [S]^n)$, where v is the reaction velocity, n is the Hill coefficient, K' is the apparent dissociation constant, allowing the parameters n, K' and V_{max} to float. Alternatively, data were modelled by a two-site, ordered-binding equation, $v = (V_{max}[S]^2/\alpha K_S^2)/(1 + [S]/K_S + [S]^2/\alpha K_S^2)$, allowing the parameters α, K_S and V_{max} to float. To compare the Michaelis–Menten model with the ordered-binding model, the F-test statistic was calculated according to the GRAPHPAD PRISM manual using the following equation: $F = ((SS_{null} - SS_{alt})/(DF_{null} - DF_{alt}))/(SS_{alt}/DF_{alt})$, where `null' and `alt' refer to the Michaelis–Menten and ordered-binding models, respectively; SS is the absolute sum of squares of the variance for each model; and DF is the number of degrees of freedom for each

model. For the Michaelis–Menten model, SS and DF were 3.564×10^7 and 68, respectively. For the ordered-binding model, SS and DF were 3.579×10^7 and 67, respectively.

Supplementary Material

Refer to Web version on PubMed Central for supplementary material.

Acknowledgements

We thank T. Pan and R. Hibbs for comments and L. Vaskalis for assistance with figures. C.L.P. was supported by the ARCS foundation and NIH training grant T32 DK007680. This work was supported by the NIH. E.G. is an investigator with the Howard Hughes Medical Institute.

References

1. Abramson J, Wright EM. Structure and function of Na^+-symporters with inverted repeats. Curr. Opin. Struct. Biol. 2009; 19:425–432. [PubMed: 19631523]
2. Krishnamurthy H, Piscitelli CL, Gouaux E. Unlocking the molecular secrets of sodium-coupled transporters. Nature. 2009; 459:347–355. [PubMed: 19458710]
3. Sobczak I, Lolkema JS. Structural and mechanistic diversity of secondary transporters. Curr. Opin. Microbiol. 2005; 8:161–167. [PubMed: 15802247]
4. Hahn MK, Blakely RD. Monoamine transporter gene structure and polymorphisms in relation to psychiatric and other complex disorders. Pharmacogenomics J. 2002; 2:217–235. [PubMed: 12196911]
5. Amara SG, Sonders MS. Neurotransmitter transporters as molecular targets for addictive drugs. Drug Alcohol Depend. 1998; 51:87–96. [PubMed: 9716932]
6. Celik L, Schiøtt B, Tajkhorshid E. Substrate binding and formation of an occluded state in the leucine transporter. Biophys. J. 2008; 94:1600–1612. [PubMed: 18024499]
7. Rosenberg A, Kanner BI. The substrates of the gamma-aminobutyric acid transporter GAT-1 induce structural rearrangements around the interface of transmembrane domains 1 and 6. J. Biol. Chem. 2008; 283:14376–14383. [PubMed: 18381286]
8. Vandenberg RJ, Shaddick K, Ju P. Molecular basis for substrate discrimination by glycine transporters. J. Biol. Chem. 2007; 282:14447–14453. [PubMed: 17383967]
9. Faham S, et al. The crystal structure of a sodium galactose transporter reveals mechanistic insights into Na^+/sugar symport. Science. 2008; 321:810–814. [PubMed: 18599740]
10. Weyand S, et al. Structure and molecular mechanism of a nucleobase-cationsymport-1 family transporter. Science. 2008; 322:709–713. [PubMed: 18927357]
11. Shaffer PL, Goehring A, Shankaranarayanan A, Gouaux E. Structure and mechanism of a Na^+-independent amino acid transporter. Science. 2009; 325:1010–1014. [PubMed: 19608859]
12. Gao X, et al. Structure and mechanism of an amino acid antiporter. Science. 2009; 324:1565–1568. [PubMed: 19478139]
13. Fang Y, et al. Structure of a prokaryotic virtual proton pump at 3.2Å resolution. Nature. 2009; 460:1040–1043. [PubMed: 19578361]
14. Yamashita A, et al. Crystal structure of a bacterial homologue of Na^+/Cl^-dependent neurotransmitter transporters. Nature. 2005; 437:215–223. [PubMed: 16041361]
15. Singh SK, Piscitelli CL, Yamashita A, Gouaux E. A competitive inhibitor traps LeuT in an open-to-out conformation. Science. 2008; 322:1655–1661. [PubMed: 19074341]
16. Shi L, et al. The mechanism of a neurotransmitter:sodium symporter-inward release of Na^+ and substrate is triggered by substrate in a second binding site. Mol. Cell. 2008; 30:667–677. [PubMed: 18570870]
17. Christensen JJ, Hill JO, Izatt RM. Ion binding by synthetic macrocyclic compounds. Science. 1971; 174:459–467. [PubMed: 17745729]

18. Kawate T, Gouaux E. Fluorescence-detection size-exclusion chromatography for precrystallization screening of integral membrane proteins. Structure. 2006; 14:673–681. [PubMed: 16615909]
19. Quick M, Javitch JA. Monitoring the function of membrane transport proteins in detergent-solubilized form. Proc. Natl Acad. Sci. USA. 2007; 104:3603–3608. [PubMed: 17360689]
20. Hansen SB, et al. Tryptophan fluorescence reveals conformational changes in the acetylcholine binding protein. J. Biol. Chem. 2002; 277:41299–41302. [PubMed: 12235129]
21. Singh SK, Yamashita A, Gouaux E. Antidepressant binding site in a bacterial homologue of neurotransmitter transporters. Nature. 2007; 448:952–956. [PubMed: 17687333]
22. Zhou Z, et al. LeuT-desipramine structure reveals how antidepressants block neurotransmitter uptake. Science. 2007; 317:1390–1393. [PubMed: 17690258]
23. Hill AV. The combinations of haemoglobin with oxygen and with carbon monoxide. I. Biochem. J. 1913; 7:471–480. [PubMed: 16742267]
24. Segel, IH. Enzyme Kinetics: Behavior and Analysis of Rapid Equilibrium and Steady-State Enzyme Systems. Wiley; 1975. p. 398-401.
25. Wiseman T, Williston S, Brandts JF, Lin LN. Rapid measurement of binding constants and heats of binding using a new titration calorimeter. Anal. Biochem. 1989; 179:131–137. [PubMed: 2757186]

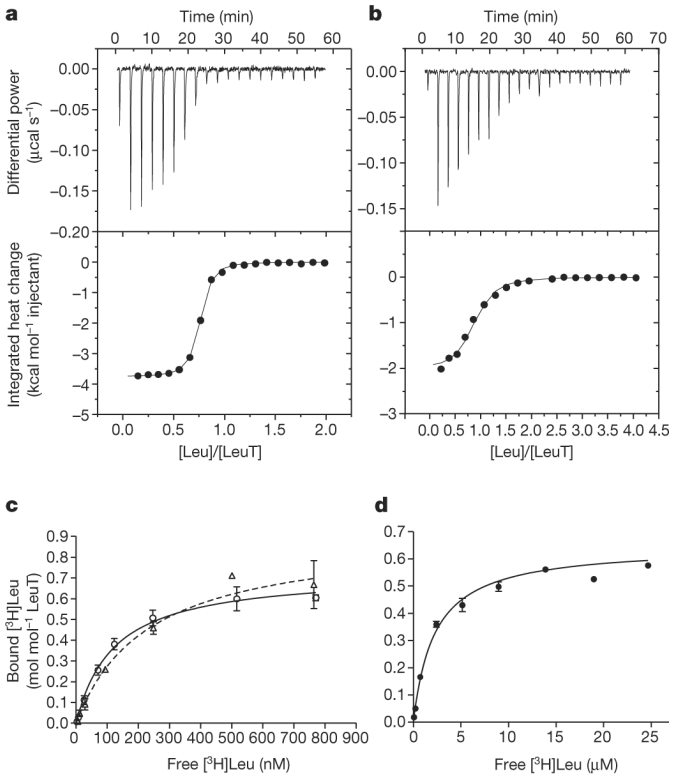

Figure 1. Leu binding measured by ITC and equilibriumdialysis

a, b, ITC data for Leu binding to wild-type LeuT (**a**) and Leu binding to mutant Tyr 108 Phe–LeuT^{K} (see Methods) (**b**). Raw injection heats (expressed as differential power) are shown in the top panels and the corresponding specific binding isotherms (calculated from the integrated injection heats and normalized to moles of injectant) are shown in the bottom panels, determined at 25 °C and pH 7.0. Square brackets denote concentration. **c, d**, Quantitation of [^{3}H]Leu-binding stoichiometry by equilibrium dialysis for the wild type (open circle, solid line) or the Leu 400 Ala mutant (open triangle, dashed line) (**c**), and for Tyr 108 Phe-LeuT^{K} (**d**). Errors bars, s.e.m.; $n = 2$.

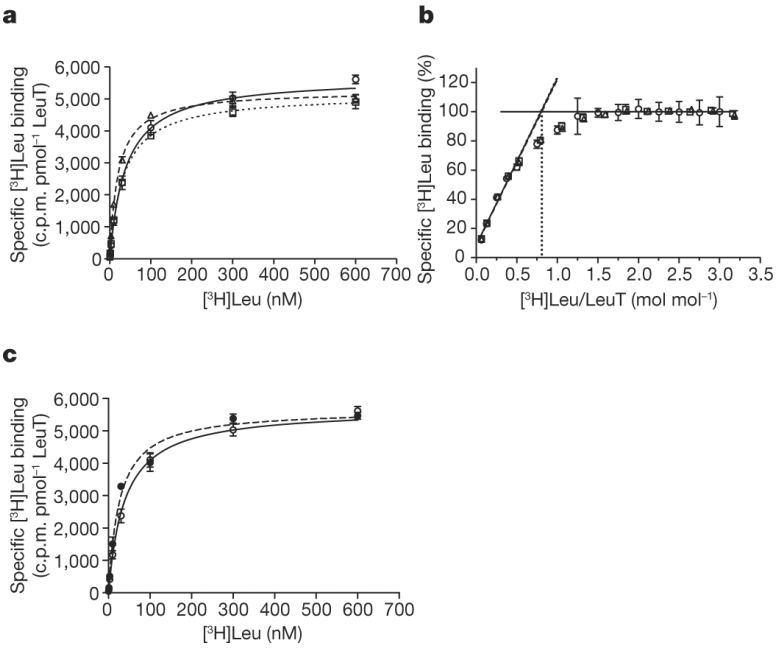

Figure 2. Leu binding measured by scintillation proximity assays

a, Saturation binding isotherms and nonlinear regression analysis for wild-type LeuT (open circle, solid line), Leu 400 Ala mutant (open triangle, dashed line) and Leu 400 Cys mutant (open square, dotted line). c.p.m., counts per minute. **b**, Saturation binding at high LeuT concentration (~20K_d), quantifying substrate-binding stoichiometry. Symbols and lines are as in **a. c**, Saturation binding for wild-type LeuT in the absence (same data as in **a**) or presence of 1mM clomipramine (closed circle, dashed line). Error bars, s.e.m.; $n = 2$.

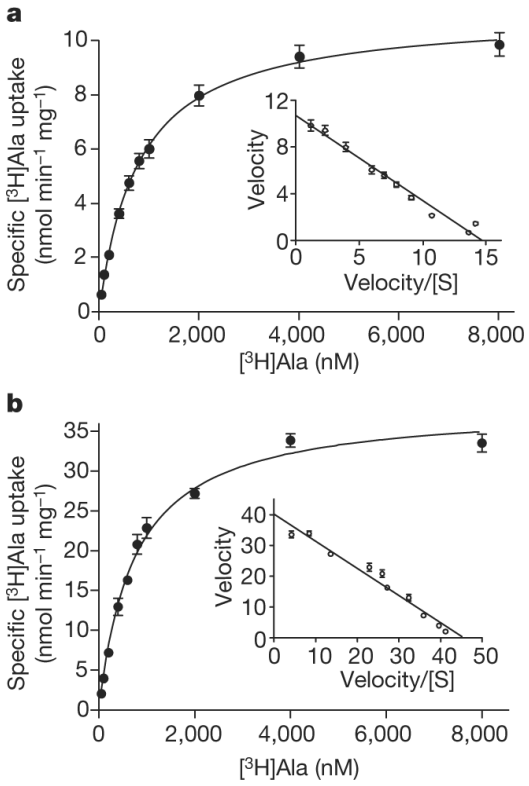

Figure 3. Transport kinetics of [^{3}H]Ala uptake

a, Steady-state Ala uptake as a function of Ala concentration at pH 5. Inset, the corresponding Eadie–Hofstee plot with linear regression (r^2 = 0.93). Error bars, s.e.m.; n = 4. *b*, Steady-state Ala uptake at pH 5 in the presence of valinomycin to induce a membrane potential. Inset, the corresponding Eadie–Hofstee plot with linear regression (r^2 = 0.96). Error bars, s.e.m.; n = 2. S, substrate.

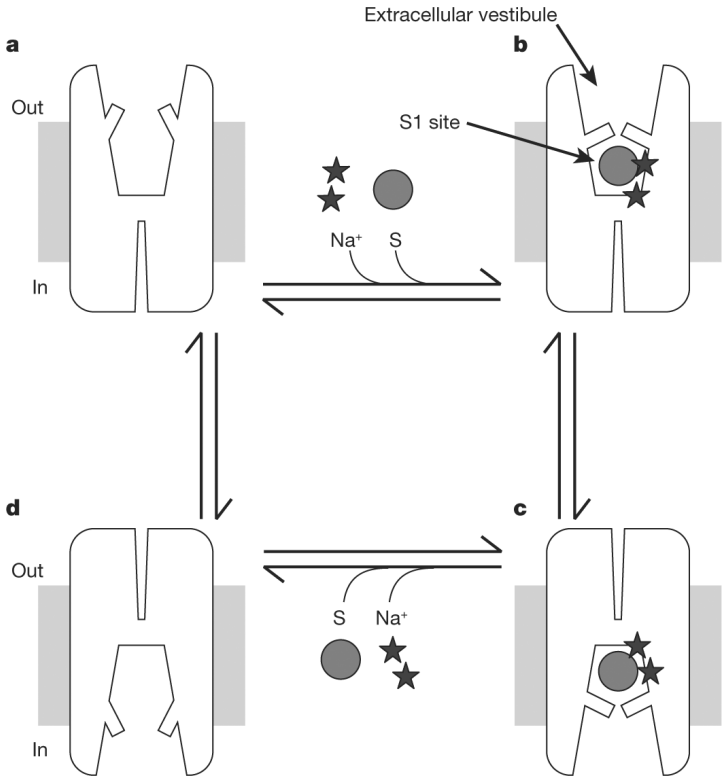

Figure 4. LeuT mechanism

Starting fromthe apo transporter in an open-tooutside conformation (**a**), substrate (S) and sodium ions bind, forming the outward-facing occluded conformation (**b**) characterized by closure of a `thin gate' over the S1 substrate-binding site[2]. Clomipramine, which inhibits transport, binds in the extracellular vestibule[21,22] directly above the thin gate, near the putative S2 site[16]. The substrate- and ion-bound transporter undergoes structural isomerization to form the inward-facing conformation (**c**), allowing release of substrate and ions to the intracellular solution, thereby generating an open-to-inside apo transporter (**d**) that isomerizes to the open-to-outside conformation (**a**).